Association of Adhesive Spheres Formed by Hydrophobically End-Capped PEO. 2. Influence of the Alkyl End-Group Length and the Chain Backbone Architecture

Fabrice Laflèche, Taco Nicolai,* and Dominique Durand

Polymères, Colloïdes, Interfaces, UMR CNRS, Université du Maine, 72085 Le Mans Cedex 9, France

Yves Gnanou and Daniel Taton

Chimie des Polymères Organiques, UMR CNRS, ENSCP, Université de Bordeaux, 33607 Talence Cedex, France

Received July 8, 2002; Revised Manuscript Received November 7, 2002

ABSTRACT: We studied the effect of the length of alkyl end groups and chain backbone architecture on the associative properties of end-capped PEO. The latter was done by comparing linear and star PEO with the same hydrophilic−lypophilic balance. With increasing length of the end groups the association number (p) of the polymeric micelles increases and the critical association concentration decreases, but these parameters are not influenced by the chain backbone architecture. The polymeric micelles behave as adhesive spheres if p is sufficiently large, which explains the phase behavior and the light scattering results. The critical concentration where the spheres percolate varies little with the length of the end groups and the architecture. At a given concentration the viscosity increases with increasing length of the end groups because the lifetime of the end groups in the multiplet increases. The chain backbone architecture has little influence on the viscoelastic properties.

Introduction

Hydrophobically end-capped poly(ethylene) oxide (PEO) is a much used model system for associative polymers.[1−12] Associative polymers have a soluble chain backbone but contain functional groups that associate, which leads to interesting rheological properties that are useful in technological applications. Polymers that contain end groups at one or both chain ends form polymeric micelles above the critical association concentration (cac) with the functional end groups situated in the central multiplet. However, if both ends are functionalized, the chains can also bridge between two multiplets and can cause the micelles to aggregate. At higher concentrations the process of bridging can lead to the formation of a transient gel but may also induce macroscopic phase separation.[11,13]

In the accompanying paper,[14] we reported a study of the phase behavior and the associative properties of PEO end-capped with hexadecyl on one or both ends, but with the same hydrophilic−lypophilic balance (HLB). We showed how the phase diagram and the light scattering results could be explained by a model of adhesive spheres. The PEO chains form micelles with size and molar mass that are practically independent of the fraction of difunctionalized PEO (f). The attraction between the micelles is caused by bridging of the difunctionalized chains. Phase separation can be induced by increasing either f or the temperature. In the first case we increase the amount of bridging, while in the latter we reduce the repulsive excluded-volume interaction between the micelles. Semiquantitative agreement between model predictions and the experimental results was obtained using an adhesion parameter that depends on the number of alkyl end groups per micelle (p), the fraction of difunctionalized chains, and the effective volume of the micelles.

Dynamic mechanical properties were characterized by two transitions. When increasing the PEO concentration, one observes at C_p a sudden rise of the viscosity. This rise was interpreted in terms of the formation of a transient gel of connected micelles. The transient gel is characterized by a relaxation time that varies weakly with the concentration and has an Arrhenius temperature dependence. The relaxation is attributed to the escape of an end group from the multiplet. The elastic modulus at high frequencies is almost independent of the temperature and increases sharply at C_p to a value close to that expected for a system in which all difunctionalized PEO act as elastic network chains. At higher concentrations a second transition occurs at C_{hg} that is characterized by a dramatic increase of the terminal relaxation time. C_{hg} is almost independent of f but increases with decreasing temperature. The transition is caused by jamming of close-packed micelles and is also observed for diblock copolymers.[15] Relaxation of the bridges is still clearly visible, but it no longer leads to full relaxation of the shear modulus. Complete relaxation of the shear modulus involves hopping or complete restructuring of the micelles, which is extremely slow.

Here we extend our earlier investigation by studying the influence of the length of the end-capped alkyl group between 10 and 18 carbons, keeping the molar mass constant (5 kg/mol per hydrophobic end group). We also studied the influence of the chain backbone architecture by comparing linear chains and starlike PEO with three and four arms, keeping the HLB constant.

Materials and Methods

Materials. Three- and four-armed star PEO was synthesized using a method described by Angot et al.,[16] and linear PEO was purchased from Fluka. The samples were characterized using static and dynamic light scattering and size exclusion chromatography (see Table 1). The polymers were functionalized with alkyl end groups using a method described

10.1021/ma0210776 CCC: $25.00
Published on Web 01/30/2003

Table 1. Characteristics of PEO Precursors

n_a	M_w (kg/mol)	M_w/M_n	R_h (nm)	$[\eta]$ (cm^3/g)
1	4.8	1.05	2.3	17
2	9.8	1.08	3.2	24
3	14.5	1.1	3.8	27
4	17.2	1.2	3.9	26

in ref 14. Size exclusion chromatography in THF showed that the functionalization had no influence on the molar mass distribution. NMR showed that within an experimental error of 5% the degree of functionalization was complete for all samples except three samples functionalized with dodecyl to a degree of 80%.

We will consider that monofunctionalized PEO has one arm and difunctionalized PEO has two arms, which means that the number of arms (n_a) of the PEO samples studied here varies between 1 and 4. If the functionalization is complete, the number of alkyl end groups per polymer is equal to the number of arms. We will use *x*C*y* to designate the samples with *x* the number of arms and *y* the number of carbons of the alkyl end group. The molar mass of each arm is approximately the same (5 kg/mol). Monofunctionalized samples (1C*y*) prepared from the commercial sample (Fluka) contain 20% (w/w) difunctionalized PEO (2C*y*) with twice the molar mass. These samples will be designated as *m*d*C*y*.

For the light scattering measurements the samples were filtered through 0.2 μm pore size Anatop filters when possible. Viscous samples were filtered through 0.45 μm pore size Millipore filters. We checked that filtration did not modify the concentration.

Methods. Fluorescence measurements were done on a Amino 500 SPF fluorescence spectrometer. The excitation wavelength was 334 nm with a bandwidth of 5 nm. The emission was measured between 350 and 600 nm with a bandwidth of 1 nm. We have determined the ratio of the first and third emission peak (I_1/I_3) of pyrene situated at 373 and 383 nm, respectively. The pyrene concentration was 6×10^{-7} M.

Dynamic mechanical and light scattering measurements were done as described in ref 14.

Results

Phase Behavior. *Influence of the Alkyl Length.* Linear PEO that is fully functionalized on both ends with an alkyl larger than C12 phase separates at room temperature into a dense gellike bottom phase and a top phase with a negligible concentration of PEO. For 2C12 phase separation occurs above 45 °C, while for 2C10 it was not observed below 80 °C. These observations agree with those reported on similar systems by Alami et al.[4] The height of the dense phase was proportional to the PEO concentration, which implies that the density of the bottom phase is independent of the total PEO concentration.

In Figure 1a we plotted the PEO concentration of the bottom phase as a function of temperature for linear PEO with different alkyl lengths. The PEO concentration of the bottom phase increases with increasing temperature. At a given temperature the density of the bottom phase decreases with decreasing alkyl length.

Homogeneous solutions can be obtained by addition of monofunctionalized PEO as was shown for 2C16 in ref 14. The critical PEO concentration is about 10 g/L and does not depend much on the temperature or on *f*. Figure 2a shows the effect of the alkyl length on the $f-T$ phase diagram at $C = 10$ g/L. More monofunctionalized PEO needs to be added to render the system homogeneous if the alkyl end group is longer except for 2C18 at high temperatures. The critical value of f (f_c) for 2C18 has a weaker temperature dependence than for 2C16 and 2C14, and at high temperatures f_c is even larger for 2C18 than for 2C16. The origin of this discrepancy will be discussed below.

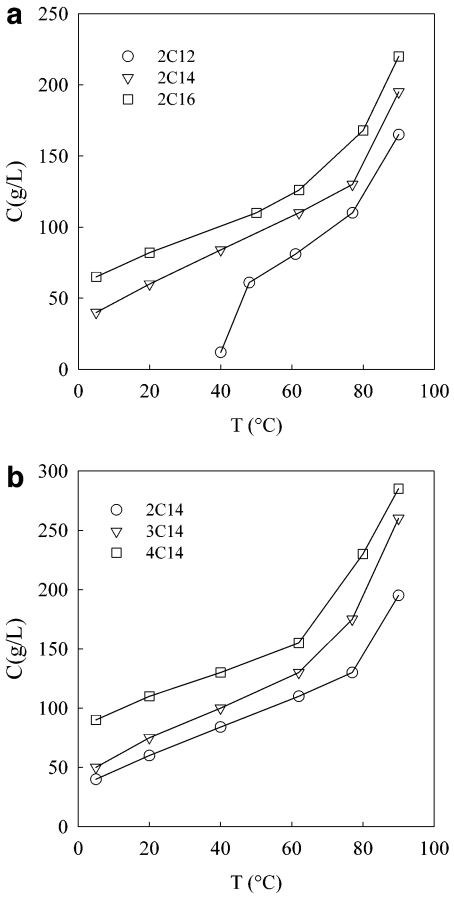

Figure 1. Temperature dependence of the concentration of the bottom phase for linear PEO end-capped with alkyl groups. (a) shows the effect of varying the length of the alkyl groups, and (b) shows the effect of varying the number of arms of the chain backbone.

Influence of the Architecture. Figure 1b shows the temperature dependence of the PEO concentration of the bottom phase for linear and star PEO end-capped with C14. At a given temperature the PEO concentration increases with increasing number of arms. This means that chain backbone architecture influences the phase behavior, because the HLB is almost the same. Figure 2b shows the effect of the architecture on the $f-T$ phase diagram at $C = 10$ g/L. Again we observe an increased tendency to phase separation if the number of arms is increased.

Fluorescence. *Influence of the Alkyl Length.* Figure 3 shows the ratio of the fluorescence peaks I_1 and I_3 of pyrene as a function of the concentration of linear PEO with $f = 0.2$ end-capped with alkyl groups of different lengths. Similar studies have been reported earlier for PEO fully end-capped at both ends.[4,18] The decrease of I_1/I_3 is caused by micelle formation and occurs at lower PEO concentrations if the length of the alkyl end group is increased. The cac, defined as the PEO concentration where I_1/I_3 starts to decrease, decreases with increasing length of the alkyl end group (see Table 2). For the samples end-capped with C16 and C18 the pyrene concentration that is necessary to obtain an accurate signal is not much smaller than the micelle concentration when I_1/I_3 starts to decrease. Therefore, the values of the cac obtained for these samples should be considered as upper limits.

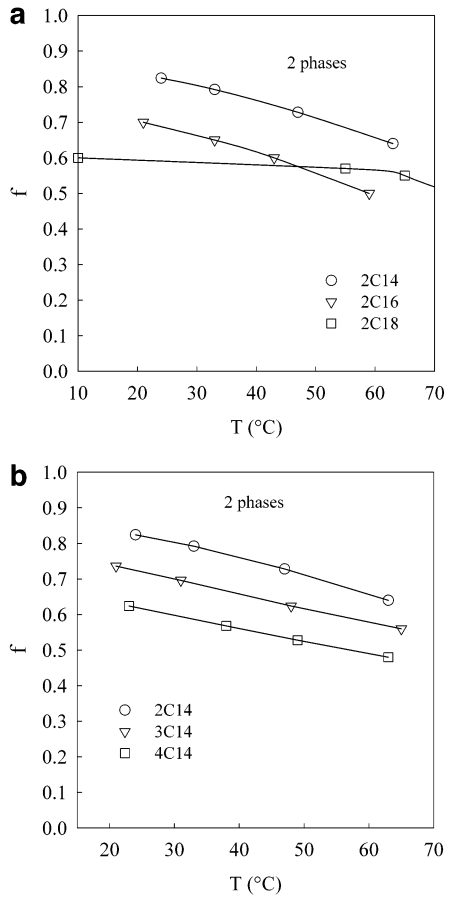

Figure 2. $f-T$ phase diagram of mixtures of PEO functionalized at all ends and monofunctionalized PEO at $C = 10$ g/L. (a) shows the effect of varying the length of the alkyl end group, and (b) shows the effect of varying the number of arms of the chain backbone. Symbols represent the temperatures where the scattering intensity diverges for fixed values of f.

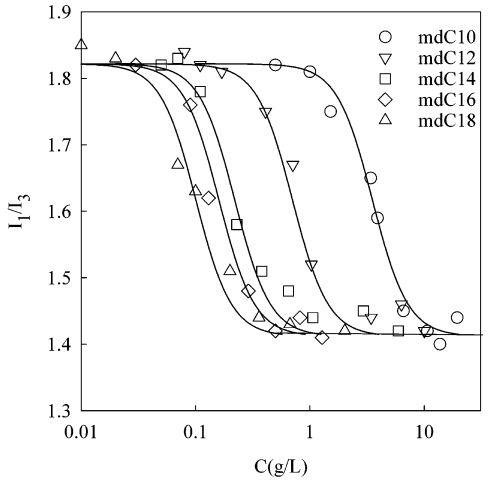

Figure 3. Dependence of the ratio of the pyrene fluorescence peaks at 373 and 383 nm on the concentration of PEO end-capped with alkyl groups of different length as indicated in the figure. Solid lines are guides to the eye.

Influence of the Architecture. To study the effect of chain architecture, we have compared 1C12, 2C12, and 3C12. The results are indistinguishable within the experimental error, which shows that the effect of chain architecture is weak if the HLB is kept the same.

Viscoelasticity. *Influence of the Alkyl Length.* We have compared the effect of alkyl length for mixtures of mono- and difunctionalized PEO with $f = 0.2$ (mdCy).

Table 2. Characteristics of Functionalized Linear PEO at 20 °C[a]

	p	R_h (nm)	C_s (g/L)	A	cac (g/L)	E_a (kJ/mol)
mdC18	43	10.3	105	2.9	0.02	46
mdC16	36	9.3	115	2.5	0.05	68
mdC14	28	8.4	120	1.6	0.13	73
mdC12	20		130	1.1	0.45	94

[a] Please note that the value of p for mdC12 and the values of the cac for mdC18 and mdC16 are only rough estimates.

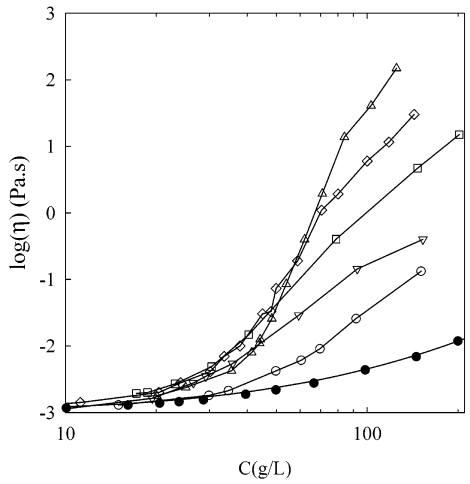

Figure 4. Concentration dependence of the viscosity at 20 °C for linear PEO end-capped with alkyl groups of different length. For comparison, the results obtained for the precursor are shown as filled symbols. Symbols are as in Figure 3.

These systems are homogeneous up until at least 80 °C over the whole concentration range. Figure 4 shows the concentration dependence of the viscosity (η) at 20 °C. Above about 40 g/L the viscosity increases strongly with increasing concentration, and the larger is the alkyl end group, the stronger is the viscosity at high concentrations. As we discussed in ref 14, the sudden rise of the viscosity is caused by the formation of a transient network when the aggregating micelles percolate the whole space. The percolation concentration (C_p) decreases if the fraction of difunctionalized PEO increases, but the effect of the alkyl length is relatively weak. The large cac of mdC10 causes the viscosity of this sample to rise at a higher concentration than the other samples.

For $C > C_p$ the viscosity has an Arrhenius temperature dependence: $\eta = \eta_0 \exp(E_a/RT)$ (see Figure 5). The activation energy is independent of the concentration for high concentrations and increases with increasing alkyl length (see Table 2). A similar variation was reported in ref 3 for HEUR, i.e., PEO end-capped with an alkyl via a urethane link. Of course, the viscosity depends on both the variation of the high-frequency plateau modulus of the transient gel (G_0) and the relaxation time (τ). For PEO end-capped with C16 the temperature dependence of G_0 is negligible, so that the temperature dependence of the viscosity is the same as that of the relaxation time. The relaxation time decreases with decreasing length of the alkyl end groups and is outside the window of observation for mdC12 and mdC14. However, the viscoelastic relaxation can be studied for mdC18 and compared with the results for mdC16 reported in ref 14.

For mdC18 we have measured the frequency dependence of the loss (G'') and storage (G') shear modulus at different temperatures between 10 and 40 °C. The data at different temperatures can be superimposed on

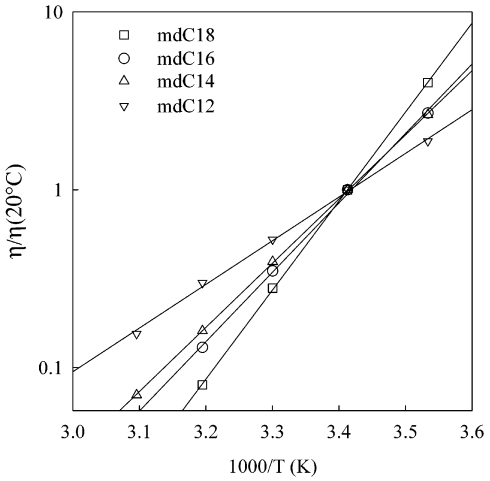

Figure 5. Arrhenius plot of the temperature dependence of the viscosity relative to that at 20 °C for linear PEO with different alkyl end groups. The solid lines represent linear least-squares fits.

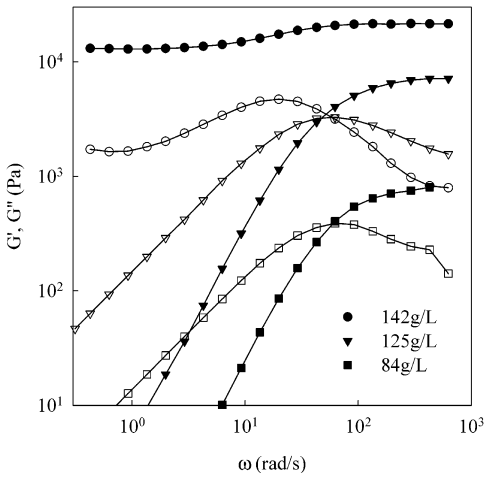

Figure 6. Angular frequency dependence of the loss (open symbols) and storage (filled symbols) shear modulus for mdC18 at three concentrations as indicated in the figure.

those at 20 °C by vertical and horizontal shifts, which shows that the relaxation time distribution is independent of the temperature. Figure 6 shows the results at 20 °C for three concentrations. Below 130 g/L the system has a liquidlike behavior at low frequencies while at high frequencies G' becomes frequency independent with a plateau value G_0. G_0 decreases weakly with increasing temperature but has a strong concentration dependence. The relaxation is characterized by a narrow relaxation time distribution. The characteristic relaxation time taken as $\tau = 1/\omega_{max}$ increases weakly with increasing concentration but has a strong temperature dependence. Just like the viscosity, it can also be characterized by an activation energy: $E_a = 82$ kJ/mol. The temperature dependence of τ is slightly smaller than that of η, because the temperature dependence of G_0 is not negligible, contrary to that for mdC16. The absolute values of τ are systematically about a factor of 10 larger for mdC18 than for mdC16.

If we assume that the origin of G_0 is the rubber elasticity of the bridging chains, then $G_0 = \nu RT$ for affine deformation with ν the molar concentration of elastically active chains and R the gas constant. If n is the molar concentration of difunctionalized chains, then $G_0/nRT = \nu/n$ is the fraction of difunctional chains that is elastically active. In Figure 7, we compare the

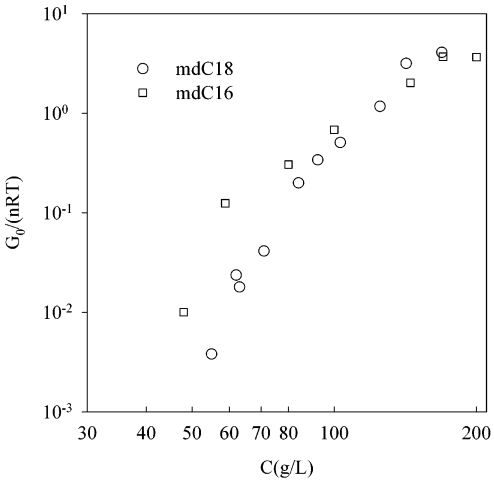

Figure 7. Comparison of the concentration dependence of the high-frequency storage modulus at 20 °C for mdC18 and mdC16.

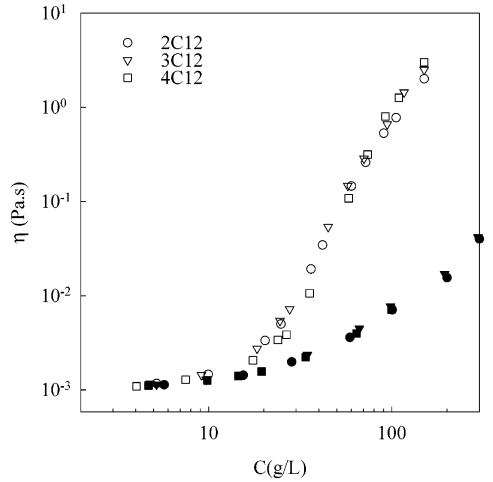

Figure 8. Comparison of the concentration dependence of the viscosity of linear and star PEO end-capped with C12 to a degree of 80% at 20 °C. The results obtained for the precursor are shown as filled symbols.

concentration dependence of G_0/nRT with that of mdC16 reported in ref 14. For both samples G_0/nRT increases rapidly and stabilizes substantially above unity. Values of G_0/nRT larger than unity point to an additional contribution to G_0.

We have shown for mdC16 that at higher concentrations a second relaxation process appears with a very long relaxation time. A similar transition occurs for mdC18 between 20 and 30 °C at $C = 142$ g/L. The concentration where the transition occurs between these two temperatures increases with decreasing alkyl length: 142, 170, and 225 g/L for mdC18, mdC16, and mdC14, respectively. For mdC12 we did not observe the transition below 300 g/L.

Influence of the Architecture. We have investigated the effect of chain architecture on the viscosity by comparing two (linear)-, three-, and four-armed star PEO end-capped with C12, keeping the HLB constant. The degree of functionalization was fixed at 80% because fully functionalized star PEO end-capped with C12 phase separates at room temperature. The results are shown in Figure 8, from which it is clear that the influence of architecture on the viscosity is weak.

Static Light Scattering. Static and dynamic light scattering measurements were done at 20 °C on solu-

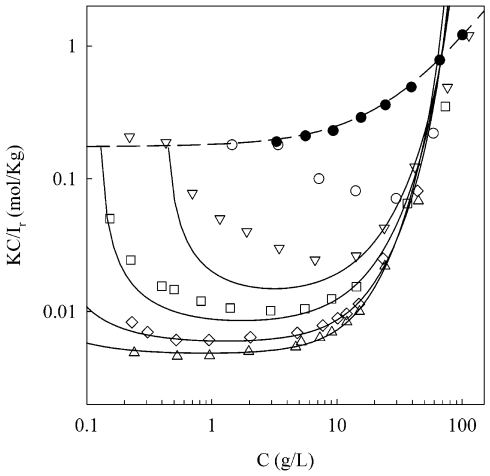

Figure 9. Concentration dependence of KC/I_r for PEO end-capped with alkyl groups of different lengths at 20 °C; symbols as in Figure 3. The results obtained for the precursor are shown as filled symbols. The dashed line represents the concentration dependence of flexible chains in good solvents predicted by renormalization group theory. The solid lines represent model predictions (see text).

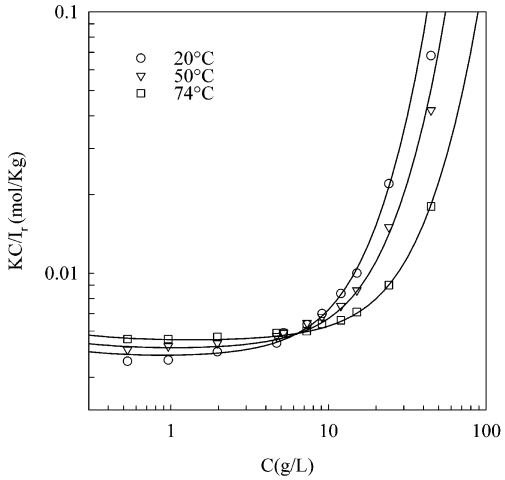

Figure 10. Concentration dependence of KC/I_r for sample mdC18 at different temperatures indicated in the figure. The solid lines represent model predictions (see text).

tions of end-capped PEO for a range of concentrations. We investigated the effect of the length of the alkyl end group by studying mixtures of mono- and difunctionalized PEO ($f = 0.2$) end-capped with alkyl groups of different length between C10 and C18. The effect of chain backbone architecture was investigated by comparing two-, three-, and four-armed star PEO ($f = 1$) that were 80% functionalized with C12. All these samples were homogeneous over the whole concentration and temperature range investigated.

We have determined the concentration dependence of KC/I_r, where I_r is the excess scattering intensity over the solvent and K is an optical constant (see ref 14). Unfiltered solutions show a contribution of spurious scattering due to the presence of a small weight fraction of aggregated material, for which we corrected as explained in ref 14. The dependence on the scattering wave vector (q) was negligible in all cases. KC/I_r is proportional to the inverse osmotic compressibility ($d\pi/dC$):[19] $KC/I_r = (d\pi/dC)/RT$, with T the absolute temperature. If interactions are negligible, KC/I_r is inversely proportional to the weight-average molar mass M_w.

Influence of the Alkyl Length. Figure 9 shows the concentration dependence of KC/I_r for PEO with alkyl end groups of different length. The results for mdC12 are close to those reported for PEO with almost the same molar mass and end-capped with dodecyl via an ether bond instead of an ester bond.[9] For comparison, we also show the results for unfunctionalized PEO. The concentration dependence for flexible linear polymers in a good solvent predicted by renormalization group theory[20] is shown by the dashed line through the data. For functionalized PEO we observe at low concentrations a decrease of KC/I_r due to the formation of polymeric micelles. As we discussed in ref 14, the effect of association of the micelles on KC/I_r of is very weak for $f = 0.2$. The onset of the decrease can be observed for mdC10 and mdC12 and occurs at slightly larger concentrations than the cac determined from pyrene fluorescence. At higher concentrations KC/I_r increases because repulsive excluded-volume interactions between the micelles become important. For all samples we observe a sharp rise of KC/I_r at $C \approx 50$ g/L, i.e., close to the concentration where the viscosity rises sharply.

For mdC18, mdC16, and mdC14 micellization occurs at low concentrations where the influence of interaction is small so that we can determine the aggregation number of end groups per multiplet (p). The results are summarized in Table 2 and show that p increases with increasing length of the alkyl groups. Pham et al.[11] reported $p = 66$ for PEO with $M_w = 35$ kg/mol end-capped on both ends with C18 via a urethane link and $p = 40$ when end-capped with C16. For mdC12 and mdC10 micellization is more gradual and is not complete before interaction becomes important. For PEO with $M_w = 10$ kg/mol end-capped with dodecyl on both ends Persson and Bales determined $p = 31$ using EPR,[21] while and Alami et al. found $p = 22$ from fluorescence decay measurements.[7]

For sample mdC18 we investigated the influence of the temperature. Figure 10 shows the concentration dependence of KC/I_r at three different temperatures. Increasing the temperature has two consequences: the aggregation number decreases ($p = 43$, 40, and 37 at 20, 50, and 74 °C, respectively), and the effect of interaction shifts to higher concentrations. The reduction of interaction is expected, because the second virial coefficient of PEO decreases with increasing temperature. On the other hand, the decrease of p with increasing temperature goes counter to the increase of hydrophobic interaction, which is the driving force for the formation of the micelles. Apparently, the reduction of the solvent quality of water for PEO with increasing temperature dominates and leads to a decrease of p for this sample. On the other hand, for mdC16 we did not observe a significant temperature dependence of p.

Influence of the Architecture. Figure 11 shows the concentration dependence of KC/I_r for two-, three-, and four-armed star PEO end-capped with C12 to a degree of 80% at $f = 1$. For $C <$ cac the values of KC/I_r are different because the molar mass of the precursors varies. The concentration where micelles begin to be formed is almost independent of the chain architecture, which confirms the results from fluorescence measurements. The decrease of KC/I_r with increasing concentration is caused by a combination of micelle formation and association of the micelles. The subsequent increase is due to excluded-volume interactions. The minimum of KC/I_r at $C \approx 10$ g/L is slightly lower if the number of arms is larger, indicating a stronger association for star PEO. However, both the position of the minimum and

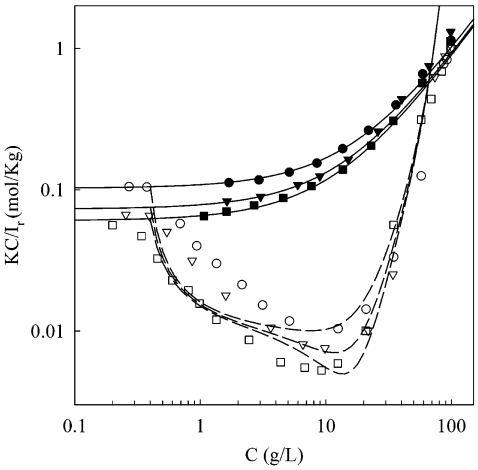

Figure 11. Concentration dependence of KC/I_r for PEO end-capped with C12 to a degree of 80% with different chain backbone architectures at 20 °C; symbols as in Figure 8. The results obtained for the precursor are shown as filled symbols. The solid lines represent the concentration dependence of flexible chains in good solvents predicted by renormalization group theory. The dashed lines are model predictions (see text).

the rise at higher concentrations are almost independent of the chain architecture.

It is clear that the dependence of p on n_a cannot be properly tested with this system, because micellization is not complete before interaction becomes important. However, we have shown in ref 14 that the molar mass of micelles formed in mixtures of PEO mono- and difunctionalized with C16 are independent of the ratio of the two components. To study the effect for star polymers, we have added three-armed star PEO end-capped with C16 (3C16) to mdC16. For this mixture we did not find a significant variation of p after addition of 3C16 to mdC16 up to an equal ratio of the two components. A higher fraction of 3C16 leads to phase separation at 20 °C.

Dynamic Light Scattering. The cooperative diffusion coefficient, D_c, was calculated from the average relaxation rate: $D_c = \langle\tau^{-1}\rangle/q^2$.[22] At higher concentrations additional slow modes are observed, and D_c was calculated from the fast mode. In all cases D_c was q-independent in the range covered by light scattering. When interactions are negligible, D_c is equal to the self-diffusion coefficient, D_s, which is related to the z-average hydrodynamic radius (R_h) as

$$D_s = \frac{kT}{6\pi\eta R_h} \qquad (1)$$

Influence of the Alkyl Length. The concentration dependence of D_c is shown in Figure 12 for mixtures of mono- and difunctionalized linear PEO ($f = 0.2$) with alkyl end groups of different length. For comparison, we also show the results for unfunctionalized precursors. The initial decrease of D_c is due to the increase of R_h from the value of unmodified PEO to that of the polymeric micelles. In ref 14 we showed that the effect of association of the micelles on D_c is very weak for $f = 0.2$. The values of R_h are summarized in Table 2 for mdC18, mdC16, and mdC14. The radius of star polymers is relatively insensitive to the aggregation number, which explains the weak variation of R_h.[23] For mdC12 and mdC10 the effect of micellization and interaction overlaps, and R_h of the micelles cannot be determined.

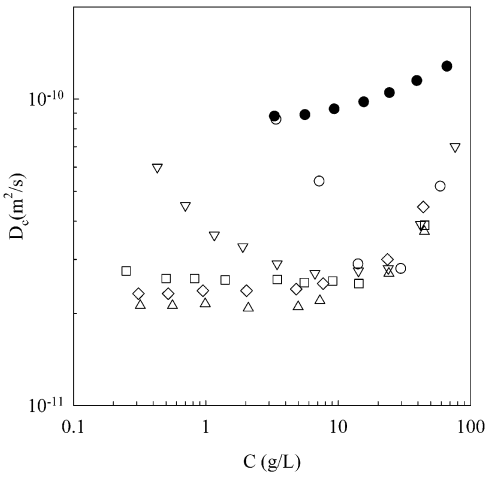

Figure 12. Concentration dependence of D_c at 20 °C for PEO end-capped with alkyl groups of different length; symbols as in Figure 3. The results for unmodified PEO are shown as filled symbols.

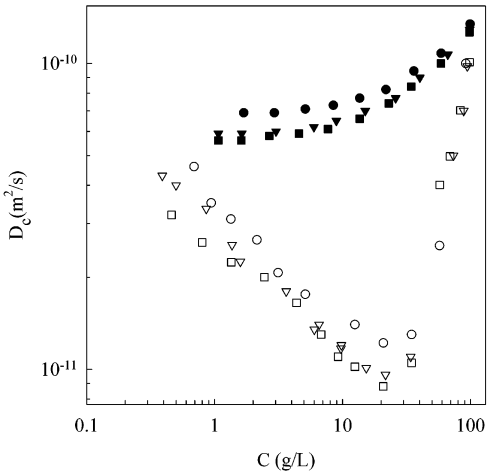

Figure 13. Concentration dependence of D_c at 20 °C for PEO end-capped with C12 to a degree of 80% with different chain backbone architecture; symbols as in Figure 8. The results for the precursors are shown as filled symbols.

At higher concentrations, the concentration dependence of D_c is determined by thermodynamic interactions and increasing friction between the micelles. The first effect leads to an increase of D_c while the latter decreases D_c. The net effect is a sharp increase of D_c at approximately the same concentration where KC/I_r and η increase sharply.

For mdC18 we measured the concentration dependence of D_c at different temperatures. Increasing the temperature leads to a weak decrease of R_h: 10.3, 9.7, and 9.1 nm at 20, 50, and 74 °C, respectively. As for the static light scattering measurements, the effect of thermodynamic interactions is shifted to higher concentrations.

Influence of the Architecture. Figure 13 shows the concentration dependence of D_c for two-, three-, and four-armed star PEO end-capped with C12 at $f = 1$. Again, the results for unfunctionalized precursors are also shown for comparison. The decrease of D_c is caused by a combination of micelle formation and association of the micelles. The subsequent increase is again due to excluded-volume interactions. The minimum is slightly lower for star PEO, which is consistent with the static light scattering results. It shows that the association is stronger if the number of arms is increased.

Discussion

Phase Behavior. In ref 14 we showed that the thermodynamics of linear end-capped PEO can be well described by a model of adhesive spheres characterized by a parameter A. The critical value of A is 10.6, assuming only binary interactions and 10.2 for the Baxter model of adhesive spheres.[24] The origin of the attraction is the gain of entropy when chain ends can exchange between neighboring multiplets. If one chain end is situated in a given micelles, the other chain end of a linear chain has two possible positions if it is at bridging distance of a second micelle. For star polymers with n_a arms $n_a - 1$ chain ends can choose between two positions. This leads to an increase of the entropy $\Delta S = k \ln(2^{n_a-1})$ per chain. In ref 14 we derived a first-order approximation of A for linear chains using mean-field theory. Including the effect of architecture, we obtain

$$A \approx \frac{v}{v_e(T)} \ln(2) f p (n_a - 1)/n_a \qquad (2)$$

where v is the true volume of the micelles and $v_e(T)$ is the effective hard-sphere volume. The temperature dependence of the latter was established in ref 14 for a commercial sample (Brij700, Aldrich) with $M_w = 4$ kg/mol that is 100% end-capped with C18 on one end via an ether link.

From eq 2 it follows that $f_c \propto v_e(T_c) n_a/(vp(n_a - 1))$. This relation explains qualitatively the variation of the $f-T$ phase diagram with the length of the end group and the architecture. At a given temperature f_c decreases with increasing length of the end group because p increases. f_c decreases with increasing number of arms because $(n_a - 1)/n_a$ increases. In ref 14 we showed that the temperature dependence of f_c for mdC16 is consistent with that of v_e, which we assumed to be the same as for Brij700. For mdC14 the temperature dependence is similar. For mdC18 the temperature dependence is different from that of v_e, because both p and v vary with the temperature. f_c has a very weak temperature dependence for this sample, because the decrease of $v_e(T)$ with increasing temperature is compensated by a decrease of p and v.

Light Scattering. The scattering results can be interpreted in terms of the model detailed in ref 14. The free energy of mixing contains a repulsive part due to excluded-volume interaction between the micelles and an attractive part due to bridging. For the repulsive interaction we used the Carnahan−Starling equation for the osmotic modulus.[25] The effect of temperature on the excluded-volume interaction can be incorporated by using a temperature-dependent effective volume fraction: $\varphi_e = C/C_s$, where $C_s = M_w/N_a v_e(T)$, with N_a Avogadro's number.

The model leads to the following expression for KC/I_r:

$$\frac{KC}{I_r} = \frac{1}{M_w}\left[\frac{1 + 4\varphi_e + 4\varphi_e^2 - 4\varphi_e^3 + \varphi_e^4}{(1-\varphi_e)^4} - 2A\varphi_e\right] \qquad (3)$$

Semiquantitative agreement was obtained for mdC16 at different f and T. However, eq 3 ignores the effect of micellization at low concentrations. If micellization is characterized by a single well-defined cac, then the weight-average molar mass of the system is given by that of the precursor $(n_a M_a)$ for $C <$ cac and for $C \geq$ cac by

$$M_w = M_a \frac{n_a \mathrm{cac} + p(C - \mathrm{cac})}{C} \quad C \geq \mathrm{cac} \qquad (4)$$

where M_a is the molar mass of a single arm.

The solid lines in Figure 9 represent eq 3 using eq 4 for M_w. The parameters used in the model predictions are summarized in Table 2. Equation 3 describes the general features of the experimental results, but the predicted decrease of KC/I_r is too abrupt for mdC12 and to a lesser extent for mdC14. The reason is that micellization of these polymers is not strictly cooperative as assumed when using eq 4. It is clear that the choice of p is rather arbitrary for these samples, especially for mdC12. For the samples with larger alkyl end groups the onset of the micellization occurs at concentrations that are experimentally inaccessible; therefore, the value of cac is uncertain. The choice of A is based on the assumption that v/v_e is the same for all samples so that A is simply proportional to p. In the calculations we have used $A = 0.07p$. We note that the parameters for mdC16 are slightly different from those used in ref 14 where we did not consider the effect of micellization.

C_s represents the concentration at which $\varphi_e = 1$ and depends on the volume fraction of the micelles, but also on the strength of exclude-volume interactions. We can estimate the volume fraction of the micelles using the hydrodynamic radius obtained from DLS: $\varphi = C4\pi R_H^3 N_a/3M_w$. The concentration at which $\varphi = 1$ varies little with the length of the alkyl end group (78, 89, and 84 g/L for mdC18, mdC16, and mdC14, respectively) and is as expected smaller than C_s. The difference between v and v_e increases with increasing temperature, i.e., with decreasing solvent quality.

Of course, KC/I_r does not diverge at C_s as predicted by the model, because the micelles can interpenetrate. In fact, as the concentration increases above C_s, the osmotic compressibility of star polymers approaches that of a semidilute solution of linear polymers.[26−28] Signs of this transition are visible in Figure 9 at $C >$ 70 g/L, i.e., when the predicted rise of KC/I_r for the micelles crosses that of linear polymers.

We found that the chain architecture has little influence on p. The model predicts that the only effect of varying n_a is to increase A. Unfortunately, it is not possible to study the effect of chain architecture for a fully functionalized system with large alkyl end groups, because they phase separate. Even for PEO end-capped with C12 we need to reduce the functionality somewhat. But for small end groups, the cac is not very low and the micellization is not fully cooperative. As a consequence, we cannot expect the model to describe the experimental results. Nevertheless, we compare in Figure 11 model predications using the same values for the cac (0.4 g/L), p (20), and C_s (130 g/L) and varying A in proportion to $(n_a - 1)/n_a$. The aim of this comparison is to show that the deeper minimum is simply a consequence of the increase of n_a.

Dynamic light scattering results are consistent with static light scattering results but are more difficult to model, because it involves the concentration dependence of the friction coefficient.

Viscoelasticity. To understand the concentration dependence of the shear modulus, we need to consider two contributions. The first contribution is the rubber elasticity of the bridging chains as discussed at length by Annable.[3] Bridging causes to association of the micelles and leads to the formation of a system spanning

network at the percolation concentration, C_p. Above C_p the viscosity and the shear modulus rise rapidly as more and more chains become elastically active. Just above C_p elastically active chains contain several micelles (so-called superbridges), which explains why the average relaxation time is less than the lifetime of a single bridge. With increasing concentration superbridges become shorter and rarer so that the average relaxation time increases.

The main effect of increasing the length of the end groups is to increase the average lifetime of a bridge and therefore the viscosity. The effect on the elastic modulus which we have only been able to compare for two samples is weak. In fact, at high concentrations where all difunctional chains are elastically active the elastic modulus is independent of the length of the end group. The percolation concentration depends on the volume fraction of the micelles and the strength of the attractive interaction. Increasing the length of the end groups leads to an increase of p and thus of the attractive interaction. However, we showed in ref 14 that the variation of C_p with A is small. In addition, the volume fraction of the micelles at a given PEO concentration depends only weakly on the alkyl length. As a consequence, C_p is almost independent of the length of the alkyl end group.

There is almost no effect of chain backbone architecture on the viscosity, because the lifetime of the bridges is the same. However, one might expect that the maximum value of the elastic modulus for star polymers is twice that of linear polymers, because for star polymers all arms become elastically active at high concentrations, while for linear chains two arms form only one elastically active chain.

The second contribution to the shear modulus is jamming of the micelles as discussed for example by Semenov et al.[13] This contribution is general for any concentrated solution of particles that cannot interpenetrate and depends on the strength of the excluded-volume interaction. It becomes important at higher concentrations and leads for PEO end-capped with C16 or C18 to systems that do not flow when tilted. The transition is rather abrupt when increasing the concentration or decreasing the temperature. The transition occurs at a lower concentration when we increase the length of the alkyl group and thus p. With increasing p the excluded-volume interaction becomes more important, leading to a transition at a lower volume fraction of the micelles. We will discuss this transition in more detail elsewhere.

Conclusions

Increasing the length of alkyl end groups leads to an increase of the aggregation number of the polymeric micelles and a decrease of the cac. The chain backbone architecture has little influence on these parameters if the HLB is kept the same.

Phase separation into a dense gellike bottom phase and a dilute top phase is more important when the length of the alkyl end group is increased or the number of arms of the chain backbone is increased.

The viscosity rises sharply at a concentration that depends weakly on the length of the alkyl end group. The increases of the viscosity is more important with increasing alkyl length. The temperature dependence is characterized by an activation energy that increases with the length of the alkyl end group. There is little effect of the chain backbone architecture on the viscosity.

The viscoelastic relaxation is characterized by a narrow relaxation time distribution. The relaxation time increases with the length of the alkyl end group, but the high-frequency shear modulus is only weakly influenced. A transition to a nonflowing system is observed over a narrow temperature decrease or concentration increase. At a given temperature the transition occurs at a lower concentration if the length of the alkyl end group is increased.

The concentration dependence of the osmotic compressibility can be described semiquantitatively with a model of adhesive spheres in which it is assumed that the adhesion parameter is proportional to the number of telechelic chains per micelles and depends on the chain backbone architecture.

References and Notes

(1) Kaczmarski, J. P.; Glass, J. E. *Macromolecules* **1993**, *26*, 5149.
(2) Yekta, A.; Xu, B.; Duhamel, J.; Adiwidjaja, H.; Winnik, M. A. *Macromolecules* **1995**, *28*, 956.
(3) Annable, T.; Buscall, R.; Ettelai, R.; Whittlestone, D. *J. Rheol.* **1993**, *37*, 695.
(4) Alami, E.; Rawiso, M.; Isel, F.; Beinert, G.; Binane-Limbele, W.; François, J. *ACS Adv. Chem.* **1996**, *248*, 343.
(5) François, J.; Maitre, S.; Rawiso, M.; Sarazin, D.; Beinert, G.; Isel, F. *Colloids Surf. A* **1996**, *112*, 251.
(6) Abrahamsén-Alami, S.; Alami, E.; François, J. *J. Colloid Interface Sci.* **1996**, *179*, 20.
(7) Alami, E.; Almgren, M.; Brown, W.; François, J. *Macromolecules* **1996**, *29*, 2243.
(8) Alami, E.; Almgren; M. Brown, W. *Macromolecules* **1996**, *29*, 5026.
(9) Chassenieux, C.; Nicolai, T.; Durand, D. *Macromolecules* **1997**, *30*, 4952.
(10) Séréro, Y.; Aznar, R.; Porte, G.; Berret, J. F.; Calvet, D.; Collet, A.; Viguier, M. *Phys. Rev. Lett.* **1998**, *81*, 5584.
(11) Pham, Q. T.; Russel, W. B.; Thibeault, J. C.; Lau, W. *Macromolecules* **1999**, *32*, 2996.
(12) Pham, Q. T.; Russel, W. B.; Thibeault, J. C.; Lau, W. *Macromolecules* **1999**, *32*, 5139.
(13) Semenov, A. N.; Joanny, J. F.; Khokhlov A. R. *Macromolecules* **1995**, *28*, 1066.
(14) Lafleche, F.; Durand, D.; Nicolai, T. *Macromolecules* **2003**, *36*, 1331.
(15) Hamley, I. W. *Philos. Trans. R. Soc. London A* **2001**, *359*, 1017.
(16) Angot, S.; Taton, D.; Gnanou, Y. *Macromolecules* **2000**, *33*, 5418.
(17) Monofunctionalized samples contain 20% difunctionalized material, which has been accounted for in the calculation of *f*. Unfortunately, the presence difunctionalized material means that star PEO samples at different *f* contain not just a fraction of monofunctionalized PEO, but also a small fraction difunctionalized PEO.
(18) Vorobyova, O.; Lau, W.; Winnik, M. A. *Langmuir* **2001**, *17*, 1357.
(19) Higgins, J. S.; Benoit, K. C. *Polymers and Neutron Scattering*; Clarendon Press: Oxford, 1994; *Light Scattering. Principles and Developments*; Brown, W.; Ed.; Clarendon Press: Oxford, 1996.
(20) Ohta, T.; Oono, Y. *J. Phys., Lett.* **1982**, *89A*, 460.
(21) Persson, K.; Bales, L. *J. Chem. Soc., Faraday Trans.* **1995**, *17*, 2863.
(22) Berne, B.; Pecora, R. *Dynamic Light Scattering*; Wiley: New York, 1976.
(23) Daoud, M.; Cotton, J. P. *J. Phys. (Paris)* **1982**, *43*, 531.
(24) Baxter, J. *J. Chem. Phys.* **1968**, *49*, 2270.
(25) Hansen, J. P.; McDonald, I. R. *Theory of Simple Liquids*; Academic Press: San Diego, 1990.
(26) Roovers, J.; Toporowski, P. M.; Douglas, J. *Macromolecules* **1995**, *28*, 7064.
(27) Witten, T. A.; Pincus, P. A.; Cates, M. E. *Europhys. Lett.* **1986**, *2*, 137.
(28) Adam, M.; Fetters, L. J.; Graessley, W. W.; Witten, T. A. *Macromolecules* **1991**, *24*, 2434.

MA0210776